



LUND UNIVERSITY

Transferability of conformational dependent charges from protein simulations

Genheden, Samuel; Söderhjelm, Pär; Ryde, Ulf

Published in:
International Journal of Quantum Chemistry

DOI:
[10.1002/qua.22967](https://doi.org/10.1002/qua.22967)

2012

[Link to publication](#)

Citation for published version (APA):
Genheden, S., Söderhjelm, P., & Ryde, U. (2012). Transferability of conformational dependent charges from protein simulations. *International Journal of Quantum Chemistry*, 112(7), 1768-1785.
<https://doi.org/10.1002/qua.22967>

Total number of authors:
3

General rights

Unless other specific re-use rights are stated the following general rights apply:
Copyright and moral rights for the publications made accessible in the public portal are retained by the authors and/or other copyright owners and it is a condition of accessing publications that users recognise and abide by the legal requirements associated with these rights.

- Users may download and print one copy of any publication from the public portal for the purpose of private study or research.
- You may not further distribute the material or use it for any profit-making activity or commercial gain
- You may freely distribute the URL identifying the publication in the public portal

Read more about Creative commons licenses: <https://creativecommons.org/licenses/>

Take down policy

If you believe that this document breaches copyright please contact us providing details, and we will remove access to the work immediately and investigate your claim.

LUND UNIVERSITY

PO Box 117
221 00 Lund
+46 46-222 00 00

Transferability of conformational dependent charges from protein simulations

Samuel Genheden, Pär Söderhjelm, Ulf Ryde

Department of Theoretical Chemistry, Lund University, Chemical Centre, P. O. Box 124,
SE-221 00, Lund, Sweden

Correspondence to

Ulf Ryde, E-mail: Ulf.Ryde@teokem.lu.se, Tel: +46 – 46 2224502, Fax: +46 – 46 2224543

2013-01-29

Abstract

We have studied the transferability of atomic charges for proteins, fitted to the quantum mechanical electrostatic potential and extensively averaged over a set of structures sampled by molecular dynamics (MD) and over all residue of the same kind in the protein sequence (xAvESP). Previously, such charges were obtained for one single protein (avidin). In this study, we employ five additional proteins. The aim of this study is fourfold. First, we provide xAvESP charges for all amino acids, including amino- and carboxy-terminal variants of all, as well as alternative protonation states of His, Asp, Glu, Lys, Arg, Cys, and Tyr. Second, we show that the xAvESP charges averaged over the five new proteins are similar to charges obtained in the same way for avidin, with a correlation coefficient of 0.997. This shows that the charges are transferable and system-independent. Electrostatic protein–ligand interaction energies calculated with charges obtained from different proteins differ by only 1–3 kJ/mol on average. The xAvESP charges correlate rather well with Amber charges (except for the N atom of amino-terminal residues), although they are obtained in a more general way. Third, the conformational dependence of the charges is significant and gives rise to quite large differences in energies. However, these differences are to a large extent screened by solvation effects. For example, the solvent-screened electrostatic interaction energy between the protein galectin-3 and five different ligands varies with the charge sets by less than 3 kJ/mol on average. Finally, we show that the xAvESP charges give a comparable root-mean-squared deviation as the Amber charges for the MD simulations of 18 protein–ligand complexes, they give comparable or slightly worse backbone N–H order parameters for two galectin-3 complexes, but they give a better correlation between calculated and experimental affinities for the binding of seven biotin analogues to avidin and for nine inhibitors of factor Xa.

Keywords: electrostatic potential charges, molecular dynamics simulations, MM/GBSA, generalised Born solvation, conformation dependence

Introduction

Molecular mechanics (MM) methods have become an important complement to experiments for the study of biochemical systems. Such methods are based upon an empirical force field, with parameters derived either from experiments or quantum mechanical (QM) calculations. One of the most important and critical part of the force field is the treatment of electrostatic interactions. In most force fields designed for simulations of macromolecules, electrostatics are treated by Coulomb interactions between partial point charges, located at the position of each atom. Naturally, the quality of the charges will strongly affect the performance of the force field.^{1,2}

One of the most common methods to obtain such atomic charges is to fit them to the electrostatic potential (ESP), calculated at a large number of points around the molecule with QM methods.^{3,4,5} However, there are two problems with such charges. First, charges on atoms that are buried by the other atoms are poorly determined, meaning that they may become unphysically large and that different charges may give fits of a similar quality.^{3,4,1} Second, it is well-known that ESP charges depend quite strongly on the conformation of the molecule.^{6,7,8,9,10} Several methods have been suggested to cure these problems, e.g. by fixing some charges,¹¹ fitting to several conformations simultaneously,^{12,13} fitting to the ESP of one conformation with restraints to the dipole moment of another molecule,² restraining the charges towards zero,^{5,14} (or to Mulliken or other less conformational-dependent charges^{15,16}), or averaging the charges obtained for different conformations.¹⁷ Alternative methods to determine geometry-dependent charges, not based on ESP fits, also exist.^{18,19} However, the only method that has been extensively employed in general-purpose macromolecular force field is the restrained ESP (RESP) method.^{5,20} This method restrains the charges toward zero, employing a hyperbolic restraint. RESP is the standard method to obtain charges in the Amber force-field family, typically using two conformations for each residue in the fitting procedure.²⁰

Recently, we performed a detailed study of the conformational dependence of ESP charges in a protein.²¹ We determined the ESP charges of each atom in the complex of the protein avidin with seven biotin analogues in 20 snapshots from molecular dynamics (MD) simulations, in total over one million charges. Thereby, we obtained a detailed picture of the conformational dependence of the charges, as well as their influence on the total electrostatic energy and the binding energy of the biotin analogues. It was concluded that the conformational dependence is significant and affects ligand-binding energies by 8–43 kJ/mol, depending on whether the ligand was charged or not. However, these effects were strongly reduced if solvation was included (e.g. to 3–7 kJ/mol for the binding energies). We showed that averaging the QM charges over the snapshots solved the buried-charge problem, but still gave energies that were close to the QM results. By averaging also over all residues anywhere in the sequence, we created a set of conformation-independent atomic charges, which we call extensively averaged ESP charges, xAvESP. The xAvESP charges were rather similar to the corresponding Amber charges ($r^2 = 0.93$), but in general somewhat larger in magnitude, indicating that the quite arbitrary restraint used in the RESP method is too large. Thus, this provides an alternative and less arbitrary method to obtain atomic charges for a protein.

However, the xAvESP charges were obtained for a restricted number of snapshots for a single protein. In this paper we investigate whether the xAvESP charges are transferable also to other proteins by calculating similar charges for five additional proteins, the carbohydrate-recognition domain of Galectin-3 (Gal3), factor Xa (fXa), hisactophilin (Hap), haloalkane dehalogenase (DhlA), and the GCN4 leucine zipper (Zip). We show that the xAvESP charges actually are transferable and confirm the conclusion reached in the previous paper. Moreover, we complement the charges with residues missing in the previous investigation. We now present xAvESP charges for all the 20 normal amino acids, including their amino- and carboxy-terminal variants, as well as alternative protonation states for His, Asp, Glu, Lys, Arg, Cys, and Tyr. We show that these charges give similar root-mean-squared deviations as the standard Amber-94 charges²² in MD simulations of several different proteins, they give better prediction of the binding affinities for seven biotin

analogues to avidin and nine inhibitors to fXa with the MM/GBSA approach, but they give slightly worse backbone NH order parameters for Gal3 with and without lactose.

Methods

The proteins

Six different proteins were considered in this study: the carbohydrate-recognition domain of galectin-3 (Gal3), factor Xa (fXa), haloalkane dehalogenase (DhlA), hisactophilin (Hap), avidin, and the GCN4 leucine zipper (Zip). The Gal3 simulations were based on two crystal structures, with two different ligands, 1kjr²³ and an unpublished structure.²⁴ The avidin simulations were based on the crystal structure 1avd,²⁵ the simulations of fXa were based on the structure 1lpk²⁶ (after removal of the ligand), those of DhlA on the structure 1ede,²⁷ and those of Zip on 2zta.²⁸ The simulations of Hap are based on an NMR structure, 1hcd.²⁹

The preparation of Gal3, fXa, and avidin has been described before,^{30,31,32} and the other proteins were prepared in a similar manner. Protons were added to the proteins assuming standard protonation states at pH 7 for all residues. In particular, all Asp and Glu residues were assumed to be negatively charged and all Lys and Arg residues were positively charged. This assignment was checked with the PROPKA software.³³ The protonation state of the His residues was decided from a detailed study of their local surroundings, solvent exposure, and hydrogen-bond networks. This study indicated that DhlA has three doubly protonated His residues (residues 37, 102, and 305) and two His protonated on N^{δ1} (residues 54 and 289). Likewise, we considered His-158 in Gal3 to be protonated on the N^{δ1} atom and the other three His residues to be protonated on the N^{ε2} atom.⁵⁷ For fXa, residues 57 and 83 were assumed to be protonated on the N^{δ1} atom, residues 91, 145, and 199 on the N^{ε2} atom, and residue 13 on both atoms.⁴³ For avidin, the single His residue in each subunit was assumed to be protonated on the N^{δ1} atom.²² Zip has a single His residue in each monomer that was assumed to be protonated on the N^{δ1} atom. Hap, finally, contains 31 His residues, which all are solvent exposed. They are known to have similar pK_a values and the protein acts as a pH sensor, binding actin only at low pH.¹¹ Therefore, we run three separate simulations of Hap, one with all His residues doubly protonated, one with all His residues protonated on the N^{ε2} atom, and one with all His residues protonated on the N^{δ1} atom. The three simulations will be called Hip, Hie, and Hid in the following.

We considered five synthetic ligands bound to Gal3 for both crystal structures. Following Sörme et al.,²⁹ they are called Lig2 to Lig6 and they are shown in Figure 1. The 1kjr crystal contains Gal3 in complex with Lig3, whereas the unpublished structure involves the complex with Lig2. We also considered the binding of biotin (Btn1) and six biotin analogues (Btn2 to Btn7) to avidin. These seven ligands are also shown in Figure 1. The six biotin analogues were manually built into the active site, based on the crystal structure with biotin,²³ as has been described earlier.^{22,57} Finally, we also considered the binding of nine inhibitors to fXa, C9–C125, shown in Figure 1.⁵⁶

The proteins were described with the Amber 99SB force field,³⁴ the biotin analogues with the Amber 99 force field,²² and the Gal3 and fXa ligands with the generalised Amber force field,⁵⁷ all using charges determined with the RESP procedure,⁵⁰ based on electrostatic potentials calculated at the HF/6-31G* level.^{22,57} The proteins were immersed in an octahedral box of TIP4P–Ewald waters³⁵ extending at least 8 Å from the protein.

MD simulations

The simulations were run by the Amber 10 sander module.³⁶ In all simulations, the SHAKE³⁷ algorithm was used to constrain the bond length involving hydrogen atoms. The temperature was kept constant at 300 K using a Langevin thermostat³⁸ with a collision frequency of 2.0 ps⁻¹, and the pressure was kept constant at 1 atm using a weak-coupling isotropic algorithm with a relaxation

time of 1 ps.³⁹ Long-range electrostatics were handled by particle-mesh Ewald summation,⁴⁰ with a fourth-order B-spline interpolation and a tolerance of 10^{-5} . The non-bonded cut-off was 8 Å and the non-bonded pair list was updated every 50 fs. The MD time step was 2 fs.

The simulation protocol for Gal3, DhIA, fXa, Hap, and Zip were as follows: The systems were energy minimised for 500 cycles of steepest descent, with all atoms, except water molecules and hydrogen atoms, restrained to their start position with a force constant of 418 kJ/mol/Å². This was followed by a 20-ps *NPT* simulation with the same restraints and a 1000-ps unconstrained *NPT* simulation. Finally, 20 independent simulations were started from this equilibrated system by using different starting velocities. These simulations were equilibrated for another 100 ps in the *NPT* ensemble. The last snapshot from this trajectory was used to obtain charges, resulting in 20 snapshots for each system.

Charge calculations and charge sets

QM charges were calculated for all atoms in all 20 snapshots of each protein (using two crystal structures for Gal3 and three different protonation states for Hap) in the same way as was described previously for avidin:¹³ The protein was divided into dipeptides (i.e. each residue was capped by CH₃CO– and –NHCH₃ groups) and the charges were calculated for these using the Merz–Kollman (MK) scheme.³⁶ The ESP charges of the capping groups were then discarded, whereas the charge on the CA atom was adapted so that the whole residue had the proper integer charge. The calculations were run with the Gaussian 03 software,⁴¹ using the Hartree–Fock (HF) method and the 6-31G* basis set. Therefore, the charges are compatible with the Amber 1994 and 1999 force fields,^{14,42} besides the fact that the Amber charges are restrained towards zero with a hyperbolic restraint, according to the RESP approach.⁵⁰ This restraint is used to suppress the charges of buried atoms and to reduce the conformational dependence of the charges. However, at the same time the fit to the ESP becomes worse.²⁵ We have previously shown that averaging over a large number of snapshots and occurrences of the same type of atom in the protein sequence has a similar effect of suppressing buried charges and reduce the conformational dependence.¹³

The calculations took ~3 CPU-minutes per residue on average. DhIA contains 4861 atoms, fXa 4427 atoms, Gal3 2283–2300 (depending on the ligand), Hap 1821–1852 atoms (depending on the protonation state), and Zip 1076 atoms. Therefore, we calculated in total 928 100 individual charges. This set of raw ESP charges will be called the QM charges in the following.

In this paper, we will also discuss five additional sets of charges. The first set was created by simply averaging the QM charges of each protein atom over the 20 snapshots, or in the case of Gal3, over 100 snapshots (20 snapshots for 5 ligand). This will be called the Aver set.

Next, we created three sets of charges by averaging the charges of the same atoms in the same amino acid, anywhere in the protein sequence, as we also did for avidin in our previous investigation.¹³ We call these charges extensively averaged ESP charges (xAvESP). The previously determined charge set for avidin is called xAvESP0. Another set of such charges, xAvESP1, was obtained by averaging over all simulations of DhIA, fXa, Gal3, Hap and Zip, whereas in a third set, xAvESP2, the avidin simulations were also included in the average. When calculating these averages, we need to use a proper weighting scheme that takes into account the differing number of residues of each type in the proteins, the different number of simulations of each protein, etc. First, xAvESP charges were determined for each protein separately by a simple average over all simulations, snapshots, and residues of each kind, i.e. with the same weight to each set of charges (this is xAvESP0 for avidin, for example). For Gal3, a single set of charges was obtained by including the simulations started from the two crystal structures in the same average. For Hap, the xAvESP charges for all residues, except the three His variants were averaged over the three simulations with Hid, Hie, and Hip. Next, the final charges were obtained by averaging over the five (xAvESP1) or six (xAvESP2) proteins, weighting with respect to the number of independent occurrences of each amino acid in the proteins. For example, each avidin monomer contains one

His and 21 Thr residues, whereas the corresponding numbers for Hap are 31 and 6. Therefore, in the averages of His charges, avidin gets a weight of 1 and Hap a weight of 31, whereas for the Thr charges, avidin gets a weight of 21 and Hap a weight of 6. These residue numbers are shown in Table 1.

Finally, we also compare with the original Amber 1994 charges.¹⁴ In this set, which is called Amber below, there is one charge for each symmetrically distinct atom in each amino acid. The six sets of charges are summarised in Table 2.

MM/GBSA calculations

The binding free energy of seven biotin analogues to avidin and nine inhibitors to fXa (Figure 1) was estimated with the MM/GBSA method.^{43,44} This method estimates the free energy of the ligand, the protein and the complex as a sum of four terms

$$G = \langle E_{MM} \rangle + \langle G_{solv} \rangle + \langle G_{np} \rangle + T \langle S_{MM} \rangle \quad (1)$$

where E_{MM} is the MM energy of the molecule, i.e., a sum of internal energies, van der Waals interactions and electrostatic interactions. G_{solv} is the polar solvation energy, estimated by the generalised Born method of Onufriev et al., model I (GB^{OBCL}), i.e. with $\alpha = 0.8$ $\beta = 0$, and $\gamma = 2.91$.⁴⁵ G_{np} is the non-polar solvation energy, estimated from the solvent-accessible surface area (SASA), using the formula $G_{np} = 0.0227 \text{ SASA (in } \text{Å}^2) + 3.85 \text{ kJ/mol}$.^{22,30,46} T is the absolute temperature and S_{MM} is an entropy estimate at the MM level. The entropy was estimated on a truncated and buffered system, as described previously,⁴³ to improve the statistical precision of the estimate. All the terms in Eqn. (1) were averages over 40 snapshots from 20 (avidin) or 40 (fXa) independent MD simulations and to obtain stable energies, the same geometry was used for all three reactants.⁴⁷ Thereby, the internal energies cancel in E_{MM} . The binding free energy, ΔG_{bind} , is then taken as the difference $G(PL) - G(P) - G(L)$, where PL is the protein–ligand complex, P is the protein and L is the ligand.

The MD snapshots for the avidin/biotin systems were generated in the following way:¹³ The systems were subjected to 500 cycles of steepest descent energy minimisation, with all atoms, except water molecules and hydrogen atoms, restrained to their start position with a force constant of 418 kJ/mol/Å². Then, 20 independent simulations were initiated by a constrained 20-ps *NPT* simulation using different starting velocities, followed by a 100-ps unconstrained *NPT* simulation. Finally, a 200 ps production run was performed in the *NPT* ensemble, with snapshots sampled each 5 ps, resulting in a total of 40 snapshots from each simulation. This protocol has been shown to give converged results for the avidin system.⁵⁷ The binding free energy was estimated for all four subunits of avidin, treating the other three ligands as a part of the protein.⁵⁷ The reported binding free energy is the average over the four subunits.

The MD snapshots for the fXa systems were generated in the same way as the MD snapshots used for charge calculation. However, the equilibration was followed by a 200 ps production run in the *NPT* ensemble, with snapshots sampled each 5 ps. To obtain converged results, 40 independent simulations were employed, resulting in a total of 40 x 40 = 1600 snapshots. All MM/GBSA calculations were done with the Amber 10 software.³²

To quantify the performance of the various methods, we use three different estimates: the correlation coefficient between the predicted and experimental data (r^2), the predictive index (PI),⁴⁸ and the mean absolute deviation from the best correlation line with a unity slope (i.e. after the subtraction of the mean signed difference; MAD). These measures are quite meaningless without estimates of their statistical uncertainty. They were obtained by simple simulations: The binding energy of each ligand was assigned a random number from a normal distribution, with the mean and standard deviation of the mean obtained for the estimates of ΔG_{bind} .⁵⁷ We then calculated MAD, r^2 and PI, and repeated this procedure 10 000 times. The standard deviations within these three sets are reported as the standard error of the quality descriptor. Throughout this paper, all reported statistical uncertainties are standard errors of the mean, i.e. the standard deviation divided by the

square root of the number of estimates.

Order parameters

The model-free order parameters (S^2) of all backbone N–H bond vectors were estimated for the apo and Lactose-bound states of Gal3 (Gal3-apo) and (Gal3-Lac). The S^2 of these two states have been estimated before with the use of Amber charges and the estimated S^2 have been compared to NMR data.⁴⁹ Here, we report S^2 parameters obtained from MD simulations with the xAvESP2 charges.

Both Gal3-apo and Gal3-Lac contain several residues with alternative conformations in the crystal structure. We have previously shown that the calculated S^2 parameters can be improved by taking these alternative conformations into account.⁵⁰ Therefore, they were grouped into five distinct groups and 10 permutations of the 32 possible states were taken at random as starting structures for MD simulations.³¹ The 10 independent simulations were initiated in the following way: The systems were energy minimised for 1000 steps, restraining all water molecules and heavy atoms to their start positions with a force constant of 418 kJ mol⁻¹ Å⁻². This was followed by a 20-ps equilibration with the same restrains and constant pressure, 50 ps equilibration without any restraints at constant pressure, and 400 ps equilibration at constant volume and no restraints. Finally, a 9.8-ns production run was performed, still at a constant volume.

The charges for lactose were calculated in the same way as the protein charges described above. MD snapshots were taken from our previous simulations of Gal3-Lac:³¹ 20 simulations were selected at random from the 32 independent simulations with alternative starting conformations and one snapshot was taken from each simulation after a 5 ns production run.

Order parameters were extracted using the isotropic reorientational eigenmode dynamics (iRED) approach,⁵¹ and they were calculated by averaging over 1 ns windows.³¹

Results and Discussion

We have calculated the QM Merz–Kollman ESP charges³⁶ for all atoms in Dh1A, fXa, two crystal structures of Gal3, and three variants of Hap. By averaging over proteins, snapshots, and residues, we then obtain extensively averaged ESP charges (xAvESP) for all atoms in each residue. The aim of this article is four-fold: First, we obtain xAvESP charges for all commonly observed residues in proteins. Second, we investigate the transferability of the xAvESP charges. Third, we check if the conclusions reached in our previous article¹³ are valid also for other proteins. Fourth, we compare the performance of the final xAvESP2 charges with standard Amber charges for the calculation of MM/GBSA binding energies and S^2 order parameters. In addition, the new simulations allow us also to study how the QM charges vary for the same protein in different crystal structures.

Occurrence of amino acids

One aim of this study is to ensure that we obtain QM charges for all normal residues in proteins. In our previous study, based only on avidin, no Cys (only Cyx in Cys–Cys cross-links), Hie, or Hip (i.e. His protonated on the N^{ε2} or on both N^{δ1}, and N^{ε2}) residues were available, and for some residues the statistics were rather poor.¹³ Therefore, we included Dh1A, which has four Cys residues, and Hap, which has 31 His residues. Moreover, we studied Hap with all three possible protonation states of His. Therefore, we now have between 7 (Cys) and 76 (Gly; average 45) occurrences of the various amino acids in the five proteins (considering only one subunit of avidin), cf. Table 1. In addition, the averages are based on 20 snapshots for each protein and multiple simulations of avidin, Gal3, and Hap. Therefore, the actual number of occurrences of each amino acid in this investigation (i.e. the number of distinct charges for each residue, included in the averages for the xAvESP2 charges) ranges from 340 for Cys to 13320 for Thr (average 4922). This should be enough to obtain statistically valid estimates for all normal amino acids (as will be illustrated

below).

Each protein was modelled with a positively charged amino-terminal and a negatively charged carboxy-terminal (Lys/Arg and Thr for avidin, Leu/Pro and Ile for Gal3, Arg and Thr for fXa, Met and Glu for Dh1A, and Met and Ile for Hap). They are treated as distinct residues in the investigation. Naturally, we have much more restricted statistics for those residues. Therefore, these calculations were complemented by calculations of charges on a dimer of a leucine zipper, in which the amino- and carboxy-terminal residues were systematically varied over all 22 naturally occurring residues (including Hid, Hie, and Hip), so that each amino acid occurred in each terminal of each peptide of the dimer once. Thus, the data of the terminal residues are based on averages over at least 40 charges.

Finally, we calculated charges also for neutral Asp, Glu, Lys, and Arg, as well as negatively charged Cys and Tyr, because such residues may occur inside the proteins (where the pK_a values can be significantly perturbed) or at low or high pH values. These were obtained from simulations of avidin and Dh1A at a low pH (Asp and Glu) and of Dh1A, fXa, Gal3, and Hap at a high pH (the other four residues). Only residues on the surface of the protein were changed (to avoid that the protein denaturates) and charges were only calculated for these residues. Thereby, the charges of these residues are based on averages over 140 to 960 charge sets. It should be noted that these proteins do not typically function at such low or high pH and experimental structures are not available at those pH values. However, this will not affect the aim of these simulations, which is simply to gain enough statistics over possible structures and conformations to obtain stable charges.

Comparison of xAvESP charges

The main aim of this article is to study the transferability of the xAvESP charges, i.e. charges averaged over all residues in the sequence, so that we get one charge for each atom in each amino acid, just as for the standard Amber force fields. Therefore, we will compare three sets of xAvESP charges. The first one (xAvESP0) is the old xAvESP charges obtained for avidin in our previous study (called consensus charges in that paper).¹³ The second one (xAvESP1), is based on all new simulations in this study, i.e. all calculations with Gal3, Dh1A, fXa, Hap, and Zip. The third set (xAvESP2) is the weighted average of the charges in these two xAvESP charge sets.

The xAvESP0 and xAvESP1 charge sets are very similar, as is illustrated in Figure 2. The correlation coefficient (r^2) between them is 0.997, with a perfect slope and intercept (1.00 and 0.00, respectively), and the mean absolute deviation (MAD) is only 0.02 e . 57%, of the 388 common charges, have an absolute difference less than 0.01 and only 9% have a difference larger than 0.05. 13% percent of the charges have a difference that is significant at the 95% confidence level. Eight charges differ by more than 0.1 e and these are CA of Cys (0.20 e in xAvESP1 and 0.41 e in xAvESP0), CB of Gln (-0.02 e and 0.13 e), CA of Met (-0.05 e and 0.09 e), CA of Hid (0.35 e and 0.21 e), CD of amino-terminal Arg (0.03 e and 0.15 e), CB of Tyr (-0.22 e and -0.10 e), CG of Gln (-0.25 e and -0.37 e), and NE of amino-terminal Arg (-0.64 e and -0.75 e). All of these were poorly determined in xAvESP0, because there is only one Hid, one Tyr, one amino-terminal Arg, two Cys, and two Gln residues in the avidin monomer. This shows that the xAvESP charges are transferable and system-independent.

The xAvESP2 charges provide an alternative to the Amber-94 charges.⁴⁴ They are obtained by averaging over a large number of conformations, rather than using a quite arbitrary restraint towards zero charge, as in the RESP procedure for the Amber charges. Therefore, we next compared the xAvESP2 and Amber charge sets. From Figure 3 it can be seen that they are rather similar with a correlation coefficient of 0.88 and a MAD of 0.11 e . In this case, the slope is 0.77 (intercept still 0.00), indicating that the Amber charges in general are somewhat smaller than the ESP charges, owing to the RESP restraint towards zero.

Moreover, there are a number of prominent outliers. In particular, there is a major difference for

the backbone N atoms of all amino-terminal residues, except Pro. In xAvESP2, these atoms have charges of -0.41 to $-0.76 e$, whereas in Amber, their charge is $+0.00$ to $+0.26 e$. The reason for this is most likely that the Amber charges were obtained by splicing together charges from residues with neutral termini and a CH_3NH_3^+ molecule, instead of studying models with the charged termini.⁵² Indeed, RESP calculations of $-\text{NHCH}_3$ capped amino-terminal residues, give charges much closer to the xAvESP charges than to the Amber charges. For example, Amber, RESP, and xAvESP2 give charges of $+0.13$, -0.63 , and -0.66 , respectively N in the amino-terminal Arg in fXa. This shows that the Amber charges are erroneous.

If we exclude the amino- and carboxy-terminal residues from the comparison, $r^2 = 0.92$, slope = 0.79 , and $\text{MAD} = 0.09 e$. Besides the amino-terminal N atoms, 84 atoms have a difference larger than $0.30 e$. Most of them are various carbon atoms, particularly in the different His residues. About half of the N atoms of the carboxy-terminal residues also show such a large difference.

Variation of charges in two crystal structures and in the Hap simulations

We calculated charges for Gal3 based on two crystal structures of the same protein (in complex with five different ligands). It is interesting to compare the resulting charges to get a feeling of how much they depend on the crystal structure. Since the two structures start at different residues (residue 113 or 114), we start the comparison from residue 115. We use Aver charges, i.e. charges averaged over the 20 snapshots and compare each ligand separately. The correlation coefficient between the various charge sets obtained from the two crystal structures is always over 0.99 (with slopes and incepts of 1.00 and 0.00, respectively) and the MAD is $0.02 e$, indicating that the charges are very similar. However, the largest differences are 0.3 – $0.5 e$, obtained for various CA atoms, which are well-known to be strongly affected by the buried-charge problem.^{50,13} Even smaller differences are obtained if we also average the charges obtained in the simulations of the five ligands: For this set of charges, the MAD is $0.01 e$ and the largest difference is $0.23 e$ (CA in Arg-71), showing that further averaging suppresses the buried-charge problem. For the 2195 common charges, 70% have a difference smaller than $0.01 e$ and 97% have a difference smaller than $0.05 e$. 10% of the charges have differences that are significant with 95% confidence. We can therefore conclude that starting from different crystal structures does not affect the calculated charges significantly.

A similar analysis can be performed for the three Hap simulations, excluding the His residues. The MAD between the Aver charges obtained in various calculations (averages over the 20 snapshots) is $0.03 e$ and the correlation coefficients are 0.98 with intercepts of 0.00 and slopes of 0.99–1.00. About 8%, of the 1294 common charges, have an absolute difference greater than $0.10 e$, whereas $\sim 31\%$ have a difference less than $0.01 e$. 45–50% of the differences are significant at the 95% confidence level. The largest differences are $\sim 0.5 e$, always for CA atoms. However, large differences are also observed for the CD and CG atoms of Arg-4 (up to $0.41 e$). The reason for these rather large differences is that the change in protonation state causes quite large changes in the local structure: The average RMSD over the 20 snapshots between the Hid, Hie, and Hip simulations are 2.35 ± 0.10 (Hip–Hie), 2.66 ± 0.13 (Hip–Hid), and $2.42 \pm 0.10 \text{ \AA}$ (Hid–Hie), respectively. This is appreciably larger than the RMSD between the first snapshot and the other snapshots for simulations with the same protonation state, $\sim 1.50 \text{ \AA}$ on average. On the other hand, a visual inspection shows that the general shape of the proteins is unchanged. This indicates that the protonation of (admittedly many) His residues has a larger influence on the results than starting from different crystal structures. This large change in the structure is functional: Hap is a sensitive pH sensor that binds actin only at pH below 7 through pH-dependent structural changes.⁵³ All 31 His residues are solvent-exposed and have been shown to have similar pK_a values.⁴

Relative energies

More interesting than the charges themselves are energies calculated from them. We first compared the total electrostatic energy in each protein, relative to the average energy of all snapshots. This energy is shown in Figure 4a for the Gal3–Lig2 simulation, obtained with the Amber, Aver, and the three xAvESP charge sets. The largest difference is 108 kJ/mol between the Amber and Aver set. This is ~15% of the total variation between the various snapshots. The average difference between Amber and Aver is 35 kJ/mol. The situation is similar for the other systems, but sometimes the difference between the Amber and the Aver is as large as 200 kJ/mol, e.g., in the Dh1A simulation. This is ~20% of the total variation over the individual snapshots and indicates that there might be a major difference between conformations sampled with the Amber charges and with true conformational dependent QM charges.

To see if the differences are suppressed by solvation, we added a generalised Born term (using the GB^{OBC1} method⁵¹) to the electrostatic energies. From Figure 4b (Gal3–Lig2 simulation), it can be seen that solvation reduces the variation in the relative energies by a factor of ~2, e.g. the total range is reduced from ~800 kJ/mol to ~400 kJ/mol. However, the difference between the Amber and the Aver charges is nearly unchanged, with a MAD of 28 kJ/mol and a maximum difference of 89 kJ/mol.

The difference between the other charge sets is smaller, e.g. 15 kJ/mol average difference between xAvESP2 and Aver. The xAvESP charge sets are even more similar. For example, the xAvESP0 and xAvESP1 charge sets give an average difference of only 7 kJ/mol and a maximum difference of 28 kJ/mol for the five simulations with the Gal3-Lig2 crystal structure. These differences are somewhat reduced by solvation (to 4 and 23 kJ/mol). This indicates that the xAvESP charge sets can probably be used interchangeably in conformational sampling, which is of large importance.

It is notable that the variation of the relative energies is in general larger in the new simulations than in the old avidin simulations. For example, for the Aver charges, the average variation in the avidin simulations was 417 kJ/mol, whereas it is 831 kJ/mol in the present simulations. The reason for this is probably that we in this study employed snapshots from 20 independent simulations, not from a single long simulation, which has been shown to provide a better sampling of the conformational space of the system.⁵⁷

Ligand-interaction energies

Even more interesting are the interaction energies between a ligand and the surrounding protein. Table 3 shows the difference in electrostatic interaction energy for the various charge sets, relative to the QM charges for the binding of the five ligands to Gal3. The Aver set is closest to the QM charges, with MADs of 2–4 kJ/mol and a maximum difference of 5–8 kJ/mol. The three xAvESP sets are quite similar, with MADs of 3–4 kJ/mol and with maximum differences of 8–12 kJ/mol. The Amber charges show a performance similar to that of the three xAvESP sets, but they are on average slightly worse.

We have also tested how far from the ligand it is needed to use the QM charges to obtain electrostatic interaction energies that are within 4 kJ/mol of those obtained with the true QM charges. It turns out that this distance is very short for all charge sets, between 1.7 and 1.9 Å, with an average of 1.8 Å. Figure 5 shows the convergence of the Gal3–Lig3 system in the snapshots that had the largest difference between the Amber and the QM charges. It can be seen that the energy converges once QM charges are used for the three closest residues.

We have also examined the solvent-screened interaction energies, because it has been shown that the solvation screens most of the electrostatic interaction energy and decreases the conformational dependence of the charges.^{13,54,55} We employed a simple continuum approach to take into account the effect of the solvation, viz. the MM/GBSA approach.⁴⁵ We therefore performed standard MM/GBSA calculations for the five ligands to Gal3, and estimated the polar solvation energy with

the generalised Born GB^{OBCI} method.⁵¹ In the calculations, either the correct QM charges or the approximate charges were used. To investigate the distance dependence of the solvation effect, we also employed mixed charge sets, where the charge of all residues outside a specific distance from the ligand (we used 14 distances, 2, 3, 4, 5, 6, 7, 8, 9, 10, 12, 15, 20, 25 and 30 Å) were changed to the approximate charges.

Table 4 shows the difference of the solvent-screened protein–ligand interaction energies for the Amber, Aver and the three xAvESP sets, relative to the QM set. As expected, the differences are reduced: the MAD is reduced to 2–4 kJ/mol, with little difference between the various charge sets. The maximum difference is 5–9 kJ/mol. All Gal3 ligands are neutral, and it was shown before that the screening effect is more pronounced for charged ligands.¹³

Performance of the Amber and xAvESP2 charges

Finally, we tested the new xAvESP2 charges for predicting the binding free energies of seven biotin analogues to avidin with the MM/GBSA approach.⁴⁵ A similar comparison was also made in our previous study, but owing to the rather poor precision of the protocol employed, no conclusion could be drawn regarding the accuracy.¹³ Hence, we here used a protocol that gives a statistical precision of ~ 1 kJ/mol.⁵⁷ The MD simulations were run with both the Amber and the xAvESP2 charge sets, and the MM/GBSA energies were calculated with the Amber, xAvESP0, or xAvESP2 charge sets.

In Table 5, we show the calculated binding free energies and the corresponding standard errors. It can be seen that there are only minor differences between the affinities estimated by the various methods. In fact, the only statistically significant differences are for Btn4 and Btn5 between the MM/GBSA estimates of Amber and xAvESP0/2 (with both MD simulations; 4–5 kJ/mol) and for Btn1 between the MD simulations with the Amber and xAvESP2 charges (4–6 kJ/mol). This shows that there is a large cancellation of differences in the electrostatic interaction energies in MM/GBSA, making it quite stable to differences in the charges. The absolute errors of the individual MM/GBSA estimates are similar for the three charge sets, although the errors with the Amber charge set are slightly smaller (as expected, because the Amber charges are slightly smaller in magnitude).

When comparing the MAD (relative to the experimental affinities⁵⁶) between the various MM/GBSA results, the difference between the three charge sets is within the statistical error: Independent of the charges, we obtain a MAD of $\sim 15 \pm 1$ kJ/mol. The difference in the predictive index (PI) obtained with various charge sets is also within the statistical error (0.80–0.85). However, the correlation coefficient is higher when using either of the two sets of xAvESP charges, a difference that is statistically significant with 95% confidence. The correlation coefficient is 0.60 ± 0.01 when using the Amber charges both for the MD simulations and the MM/GBSA calculations, whereas it is 0.67 ± 0.02 when simulating and calculating energies with the xAvESP2 charge set. Likewise, when simulating with Amber charges, we obtain a significantly better correlation coefficient when calculating the energies with the xAvESP2 charges (0.66 ± 0.01) than with the Amber charges (0.60 ± 0.01). This indicates that the xAvESP2 charges might be somewhat more realistic than the Amber charges for this test set.

To check if we get the same results for another system, we also calculated MM/GBSA binding affinities for the nine inhibitors of fXa in Figure 1. Again, MD simulations were performed with both the Amber and xAvESP2 charges and the MM/GBSA energies were calculated with the same two charge sets. The results are collected in Table 6 and show that the xAvESP2 charges consistently give 2–9 kJ/mol (Amber simulations) or 5–12 kJ/mol (xAvESP2 simulations) more negative binding affinities. Thus, the difference between the two charge sets is somewhat larger for fXa, most likely because all ligands have a net charge of +1 (C39, C57, C63) or +2. Moreover, xAvESP2 consistently gives lower MADs, higher r^2 , and higher PI than the Amber charges, irrespectively if the Amber and xAvESP2 simulations are considered. The differences are rather

small, but the difference in r^2 is significant at the 99% level, whereas the difference in MAD is 87% significant for the xAvESP2 simulations. This indicates that the xAvESP2 charges may be advantageous to use for MM/GBSA ligand-binding affinity estimates.

Next we calculated backbone N–H model-free S^2 order parameters for Gal3, both in the apo and the lactose-bound state. In Table 7, the results are compared to NMR data,²⁶ using eight different quality descriptors that have been found to be useful in comparison of S^2 order parameters.^{31,57} It can be seen that for 13 of the quality descriptors, the Amber charges give better results whereas for four of them the xAvESP2 charges give better results. However, the differences are small, and only in two cases are they statistically significant, viz. the median difference for Gal3-apo (95% significance) and the mean signed difference for Gal3-Lac (90% significance), in both cases with Amber giving the better results. However, considering that 22 quality estimates are used, this could actually be by chance. The probability that a certain charge set should give the best results in 13 or more out of 22 quality measures by chance is 0.14.

Finally, we studied the stability of MD trajectories obtained with the Amber and xAvESP2 charge sets by calculating the root-mean-squared deviation (RMSD) of all back-bone atoms relative to the crystal structure (possibly with a modified ligand) for all the snapshots used for calculations of the MM/GBSA free energies or the order parameters. The average RMSD over all atoms was then averaged over all trajectories, and this result and the corresponding standard error are listed in Table 8. It can be seen that the two charge sets give similar RMSDs. In six cases, the Amber charges give a significantly lower RMSD, whereas in five cases, the xAvESP2 charges give significantly lower RMSD (at the 95% level). Thus, there is no indication that any of the two charge sets gives more stable MD trajectories.

Conclusions

We have studied the transferability of the QM ESP charges, calculated for all protein atoms and averaged over 20 snapshots taken from MD simulations and over all residues of the same type in the sequence, extensively averaged ESP charges (xAvESP). To do this, we have run several MD simulations of five protein systems. The selection involves proteins that consist mainly of helices (Zip), mainly of β sheets (avidin, Hap, Gal3), or mixtures (DhlA and fXa). We have compared the new xAvESP charges with those obtained previously from similar calculations on avidin with seven different biotin analogues.¹³ Overall, we find an excellent correlation between the old xAvESP0 and the new xAvESP1 charges, with a correlation coefficient of 0.997, and a MAD of 0.02 e . The two charge sets give relative total electrostatic energies in the whole proteins that differ by 7 kJ/mol on average (4 kJ/mol if solvation effects are included) and ligand-binding energies that differ by 2 kJ/mol on average (0.5 kJ/mol if solvation effects are included). The MM/GBSA binding estimates of seven biotin analogues differ by up to 2 kJ/mol. This clearly shows that the xAvESP charges are transferable. These two xAvESP charge sets are averaged into the final xAvESP2 set.

This set of QM charges, can be seen as an alternative to the Amber 1994 charges. For the Amber charges, the RESP procedure, which restrains charges towards zero, is used to suppress the buried-charge problem and the conformational dependence. In our procedure, these problems are instead suppressed by extensive averaging over different proteins, several snapshots from MD simulations, and occurrences of the same atom type in different places in the protein sequence. Thereby, the arbitrary restraint in RESP is avoided. The present results show that our procedure is not sensitive to the selection of proteins for the average, the only arbitrary choice in our approach.

Recently, another procedure to obtain QM charges for a whole protein has been suggested, the polarised protein-specific charges.⁵⁸ This procedure also employs dipeptide fragments, but it includes charges of all the other groups in the protein, as well as surface charges, representing the solvent reaction field from a Poisson–Boltzmann calculations. Thereby, the polarising effect of the surroundings is included in these charges, making them prepolarised (but not polarisable). Thus,

they are intended to be specific and different for each residue and protein, and should therefore not be averaged. Instead, they employ the RESP procedure to suppress the buried charge problem. They include both conformational dependence and some polarisation, but they ignore dynamic effects and dynamic changes in the polarisation, because they are calculated for a single structure. Thus, they solve other problems than the present charges. The two approaches could be combined by including a point-charge model of the surroundings in the ESP fits and averaging over several snapshots.

The xAvESP2 charge set correlates quite well with the Amber charge set ($r^2 = 0.88$), but we have revealed several problems with the Amber charges, in particular concerning the amino-terminal residues. When used in simulations, the xAvESP2 charges give similar RMSDs as Amber charges in MD simulations of 18 different protein–ligand complexes. Moreover, they give better ligand affinities estimated by the MM/GBSA method for seven biotin analogues binding to avidin and for nine inhibitors binding to fXa. The differences are not very big, which is perhaps the most important results: Even if the absolute affinities obtained with the two charge sets may differ by up to 12 kJ/mol, the relative affinities differ by less than 4 kJ/mol and the MADs with less than 1 kJ/mol. Still, for both systems, the xAvESP2 charges give significantly better correlation between the calculated and experimental affinities, e.g. by 0.68 ± 0.01 compared to 0.61 ± 0.01 for avidin, and 0.61 ± 0.05 , compared to 0.41 ± 0.06 for fXa. On the other hand, the xAvESP2 charges seems to give slightly worse model-free S^2 order parameters for two Gal3 complexes than the Amber charges, although it is not fully clear whether the differences are statistically significant.

Together, these results show that the present approach to obtain atomic charges for protein simulations is promising. Without any other changes in the Amber force field, the xAvESP2 charges give better MM/GBSA ligand-binding affinities than the standard Amber charges for the two systems studied, indicating that the xAvESP2 charges give a slightly better description of the electrostatic interactions. On the other hand, the order parameters strongly depend on all part of the force field, and in particular the backbone dihedral parameters, which are strongly optimised in the Amber-99SB force field.²¹ With that in mind, it is impressive that the xAvESP2 charges, without any change in the force field still gave comparable results to the Amber charges. Therefore, we strongly believe that the procedure to obtain atomic charges described in this paper provides a competitive and less biased alternative to the RESP procedure. In particular, we recommend the xAvESP2 charges for the amino- and carboxy-terminal residues, for which the standard Amber charges do not seem to be optimal, and also for the neutral Arg and the negatively charged Tyr residues, for which Amber charges are missing. Therefore, xAvESP2 charges for all natural amino acids, as well as carboxy- and amino terminals, and alternative protonation states of His, Asp, Glu, Lys, Arg, Cys, and Tyr are provided in the supplementary material and also on our web site (<http://www.teokem.lu.se/~ulf/Methods/xavesp.html>). We urge interested users to test them.

Acknowledgements

This investigation has been supported by grants from the Swedish research council and from the Research school in pharmaceutical science. It has also been supported by computer resources of Lunarc at Lund University and HPC2N at Umeå University.

References

- 1 Bachrach, S. M. *Rev Comp Chem* 1994, 5, 171-227
- 2 Sigridsson, E.; Ryde, U. *J Comput Chem* 1998, 19, 377-395
- 3 Chirlian, L. E.; Francl, M. M. *J Comput Chem* 1987, 6, 894-905
- 4 Besler, B. H.; Merz, K. M.; Kollman, P. A. *J Comput Chem* 1990, 11, 431-439
- 5 Breneman, C., M.; Wiberg, K. B. *J Comput Chem* 1990, 11, 361-373
- 6 Williams, D. E. *Biopolymers* 1990, 29, 1367-1386
- 7 Stouch, T. R.; Williams, D. E. *J Comput Chem* 1992, 13, 622-632
- 8 Reynolds, C. A.; Essex, J. W.; Richards, W. G. *Chem Phys Lett* 1992, 199, 257-260

- 9 Shirts, R. B.;Stolworthy, L. D. *J Inclusion Phenom Mol Recognit Chem* 1995, 20, 297-321
- 10 Pacios, L. F.;Gómez, P. C. *J Mol Struct (Theochem)* 2001, 544, 237-251
- 11 Stouch, T. R.; Williams, D. E. *J. Comput. Chem.* 1993, 14, 858-866.
- 12 Reynolds, C. A.; Essex, J. W.; Richards, W. G. *J. Am. Chem. Soc.* 1992, 114, 9075-9079.
- 13 Bayly, C. I.; Cieplak, P.; Cornell, W. D.; Kollman, P. A. *J. Phys. Chem.* 1993, 97, 10269-10280.
- 14 Sigfridsson, E.; Ryde, U. *J. Comp. Chem.*, 2002, 23, 351-364.
- 15 Lévy, B.; Enescu, M. *J. Mol. Struct. (Theochem)* 1998, 432, 235.
- 16 Berente, I.; Czinko, E.; Náray-Szabó, G. *J. Comput. Chem.* 2007, 28, 1936-1942.
- 17 Basma, M.; Sundara, S.; Calgan, D.; Vernali, T.; Woods, R. J. *J. Comput. Chem.* 2001, 22, 1125-1137.
- 18 Rappé, A. K.;Goddard, W. A. *J Phys Chem* 1991, 95, 3358-3363
- 19 Dinur, U.;Hagler, A. T. *J Comput Chem* 1995, 16, 154-170
- 20 Cornell, W. D.;Cieplak, P.;Bayly, C. I.;Kollman, P. A. *J Am Chem Soc* 1993, 115, 9620-9631
- 21 Söderhjelm, P.; Ryde, U. *J Comput Chem* 2009, 39, 750-760
- 22 Cornell, W.D., Cieplak, P., Bayly, C.I., Gould, I.R., Merz, K.M., Ferguson, D.M., Spellmeyer, D.C., Fox, T., Caldwell, J.W., Kollman, P.A. 1995. *J Am Chem Soc* 117, 5179-5197.
- 23 Sorme, P., Arnoux, P., Kahl-Knutsson, B., Leffler, H., Rini, J.M., Nilsson, U.J. *J Am Chem Soc* 2005, 127, 1737-1743
- 24 Diehl, C., Engström, O.; Delaine, T.; Håkansson, M.; Genheden, S.; Modig, K.; Leffler, H.; Ryde, U.; Nilsson, U.; Akke, M. Protein flexibility and conformational entropy in ligand design targeting the carbohydrate recognition domain of galectin 3, *J. Am. Chem. Soc.*, submitted..
- 25 Pugliese, L.;Coda, A.;Malcovati, M.;Bolognesi, M. *J Mol Biol* 1993, 231, 698-710
- 26 Matter, H., Defossa, E., Heinelt, U., Blohm, P.M., Schneider, D., Mueller, A., Herok, S., Schreuder, H.A., Liesum, A., Brachvogel, V., Loenze, P., Walser, A., Al-Obeidi, F., Wildgoose, P. *J Med Chem* 202, 45, 2749-2769
- 27 Verschuere, K.H., Franken, S.M., Rozeboom, H.J., Kalk, K.H., Dijkstra, B.W. *J Mol Biol* 1993, 232, 856-872
- 28 O'Shea, Erin K., Klemm, J. D., Kim, P. S., Alber, T. *Science* 1991, 254, 539-544
- 29 Habazettl, J., Gondol, D., Wiltscheck, R., Otlewski, J., Schleicher, M., Holak, T.A. *Nature* 1992, 359, 855-858
- 30 Weis, A.; Katebzadeh, K.; Söderhjelm, O.; Nilsson, I.J. Ryde, U. *J Med Chem* 2006, 49, 6595-6606
- 31 Genheden, S.; Ryde U. *J Comput Chem* (in press); DOI: [10.1002/jcc.21546](https://doi.org/10.1002/jcc.21546).
- 32 J. Kongsted, U. Ryde, J. (2009) *Comp.-Aided Mol. Des.*, 23:63-71
- 33 Li, H.; Robertson, A. D.; Jensen, J. H. *Proteins, Struct. Funct. Bioinf.* 2005, 61, 704-721.
- 34 Hornak, V., Abel, R., Okur, A., Strockbine, B., Roitberg, A., Simmerling, C. (2006) *Proteins: Struct., Funct. Bioinform.* 65:712-725
- 35 Horn, H. W., Swope, W. C., Pitera, J. W., Madura, J. D., Dick, T. J., Hura, G., Head-Gordon, T. (2004) *J. Chem. Phys.* 120:9665-9678
- 36 D.A. Case, T.A. Darden, T.E. Cheatham, III, C.L. Simmerling, J. Wang, R.E. Duke, R. Luo, M. Crowley, R.C.Walker, W. Zhang, K.M. Merz, B. Wang, S. Hayik, A. Roitberg, G. Seabra, I. Kolossváry, K.F.Wong, F. Paesani, J. Vanicek, X. Wu, S.R. Brozell, T. Steinbrecher, H. Gohlke, L. Yang, C. Tan, J. Mongan, V. Hornak, G. Cui, D.H. Mathews, M.G. Seetin, C. Sagui, V. Babin, and P.A. Kollman (2008), AMBER 10, University of California, San Francisco.
- 37 Ryckaert, J. P, Ciccotti, G., Berendsen, H. J. C. (1977) *J. Comput. Phys.* 23, 327-341
- 38 Wu, X., Brooks, B.R. (2003) *Chem. Phys. Lett.* 381, 512-518
- 39 Berendsen, H.J.C.; Postma, J.P.M.; van Gunsteren, W.F.; DiNola, A.; Haak, J.R. *J Chem Phys*, 1984, 81, 3684–3690
- 40 Darden, T., York, D., Pedersen, L. (1993) *J. Chem. Phys.* 98, 10089-10092
- 41 Frisch, M. J.; Trucks, G. W.; Schlegel, H. B.; Scuseria, G. E.; Robb, M. A.; Cheeseman, J. R.; Montgomery, J. A., Jr.; Vreven, T.; Kudin, K. N.; Burant, J. C.; Millam, J. M.; Iyengar, S. S.; Tomasi, J.; Barone, V.; Mennucci, B.; Cossi, M.; Scalmani, G.; Rega, N.; Petersson, G. A.; Nakatsuji, H.; Hada, M.; Ehara, M.; Toyota, K.; Fukuda, R.; Hasegawa, J.; Ishida, M.; Nakajima, T.; Honda, Y.; Kitao, O.; Nakai, H.; Klene, M.; Li, X.; Knox, J. E.; Hratchian, H. P.; Cross, J. B.; Bakken, V.; Adamo, C.; Jaramillo, J.; Gomperts, R.; Stratmann, R. E.; Yazyev, O.; Austin, A. J.; Cammi, R.; Pomelli, C.; Ochterski, J. W.; Ayala, P. Y.; Morokuma, K.; Voth, G. A.; Salvador, P.; Dannenberg, J. J.; Zakrzewski, V. G.; Dapprich, S.; Daniels, A. D.; Strain, M. C.; Farkas, O.; Malick, D. K.; Rabuck, A. D.; Raghavachari, K.; Foresman, J. B.; Ortiz, J. V.; Cui, Q.; Baboul, A. G.; Clifford, S.; Cioslowski, J.; Stefanov, B. B.; Liu, G.; Liashenko, A.; Piskorz, P.; Komaromi, I.; Martin, R. L.; Fox, D. J.; Keith, T.; Al-Laham, M. A.; Peng, C. Y.; Nanayakkara, A.; Challacombe, M.; Gill, P. M. W.; Johnson, B.; Chen, W.; Wong, M. W.; Gonzalez, C.; Pople, J. A. *Gaussian 03, Revision*; Gaussian, Inc.: Wallingford, CT, 2004.
- 42 Wang, J.; Cieplak, P.; Kollman, P. A. *J. Comput. Chem.* 2000, 21, 1049-1074.
- 43 Kollman, P. A., Massova, I., Reyes, C., Kuhn, B., Huo, S., Chong, L., Lee, M., Lee, T., Duan, Y., Wang, W., Donini, O., Cieplak, P., Srinivasan, J., Case, D. A., Cheatham, T. E. (2000) *Acc. Chem. Res.* 33, 889-897
- 44 Massova, I; Kollman, P. A. (2000) *Perspect. Drug Discov. Design* 18, 113-135
- 45 A. Onufriev, D. Bashford, D. A. Case, *Proteins* 2004, 55, 383-394

-
- 46 Kuhn, B.; Kollman, P. A. *J. Med. Chem.* 2000, 43, 3786-3791.
47 Swanson, J. M. J.; Henschman, R. H.; McCammon, J. A. *Biophys J* 2004, 86, 67-74
48 Pearlman, D. A., Charifson, P. S. (2001) *J. Med. Chem.* 44:3417-3423
49 Diehl, C.; S. Genheden, K. Modig, U. Ryde, M. Akke (2009) *J. Biomol. NMR*, 45, 157-169,
50 Genheden, S.; C. Diehl, M. Akke, U. Ryde (2010) *J. Chem. Theory Comput.*, 2010, 6, 2176-2190.
51 Prompers, J. J.; Brüschweiler, R. *J. Am. Chem. Soc.* **2002**, 124, 4522-4534.
52 Cieplak, P.; Cornell, W. D.; Bayly, C.; Kollman, P. A.; *J. Comput. Chem.* 1995, 11, 1357-1377.
53 Houliston, R. S., Liu, C., Singh, L. M. R. & Meiering, E. M. (2002) *Biochemistry*. 41, 1182-1194.
54 Urban, J. J.; Famini, G. R. *J. Comput. Chem.* 1993, 14, 353-362
55 Resat, H.; Maye, P. V.; Mezei, M. *Biopolymers* 1997, 41, 73-81
56 N. M. Green, Avidin, *Adv. Protein Chem.* 1975, 29, 85-133.
57 Meiler, J.; Promper, J. J.; Peti, W.; Griesinger, C.; Brüschweiler, R. *J. Am. Chem. Soc.* **2001**, 123, 6098-6107.
58 Changge, J.; Mei, Y.; Zhang, J. Z. H. *Biophys. J.* 2008, 95, 1080-1088.

Table 1. The number of amino acids in avidin (only one subunit), fXa, Gal3, DhlA, and Hap. These numbers are the weights used for the xAvESP1 and xAvESP2 charge sets. Cyx is cystine in Cys–Cys cross-links, whereas Hid, Hie, and Hip are His protonated on the $N^{\delta 1}$, $N^{\epsilon 2}$, and on both $N^{\delta 1}$ and $N^{\epsilon 2}$, respectively.

	Avidin	fXa	Gal3	DhlA	Hap	Total
Ala	4	15	6	30	5	60
Arg	8	16	9	15	1	49
Asn	10	10	14	10	2	46
Asp	5	14	7	26	6	58
Cys	0	1	1	4	1	7
Cyx	2	14	0	0	0	16
Gln	2	12	4	13	1	32
Glu	6	21	6	18	7	58
Gly	11	26	8	18	13	76
Hid	1	2	1	2	31	37
Hie	0	3	3	0	31	37
Hip	0	1	0	3	31	35
Ile	7	14	10	14	6	51
Leu	7	15	13	28	7	70
Lys	8	19	8	12	9	56
Met	2	4	2	11	1	20
Phe	7	13	8	23	5	56
Pro	2	9	10	23	0	44
Ser	9	14	6	13	8	50
Thr	21	22	5	16	6	70
Trp	4	4	1	6	0	15
Tyr	1	10	3	11	3	28
Val	7	18	13	14	6	58

Table 2. Description of the six charge sets considered in the work.

Charge set	# Distinct charges	Description	Charges are different for		Proteins included
			Snapshots	Same residue	
QM	928	100 QM ESP charges	Yes	Yes	DhlA, fXa, Gal3, Hap, Zip
Aver	19	227 Average over snapshots	No	Yes	DhlA, fXa, Gal3, Hap, Zip
xAvESP0	596	Aver, averaged over residues	No	No	Avidin ¹³
xAvESP1	523	Aver, averaged over residues	No	No	DhlA, fXa, Gal3, Hap, Zip
xAvESP2	547	Aver, averaged over residues	No	No	Avidin, DhlA, fXa, Gal3, Hap, Zip
Amber	507	Amber FF94 charges	No	No	Amber ⁴⁴

Table 3. Mean absolute, minimum, and maximum difference (Mad, Min and Max; in kJ/mol) between the various charge sets and the QM charges for the ligand–protein electrostatic interaction energy of the simulations of Gal3 (based on the crystal structure with Lig2). A negative sign indicates that the charge set gives more negative energies than the QM charges. In addition, the average (Av) and maximum distance (Md) at which the residue-wise cumulative energy difference is converged to within 4 kJ/mol are given. The last line gives the average, minimum or maximum over all ligands.

	Amber					Aver					xAvESP0					xAvESP1					xAvESP2				
	MAD	Min	Max	Av	Md	MAD	Min	Max	Av	Md	MAD	Min	Max	Av	Md	MAD	Min	Max	Av	Md	MAD	Min	Max	Av	Md
Lig2	4.1	-9.0	10.2	1.8	2	3.8	-8.8	7.0	1.8	2	3.9	-7.5	8.1	1.8	2	3.8	-8.9	7.1	1.8	2	3.8	-8.7	7.3	1.8	2
Lig3	3.5	-3.6	11.7	1.8	2	2.4	-3.5	7.8	1.8	2	3.8	0.3	12.3	1.9	3	3.3	-1.2	10.9	1.9	3	3.3	-1.1	11.2	1.9	3
Lig4	3.7	-4.6	7.0	1.7	2	2.1	-4.7	6.5	1.7	2	3.7	-1.5	8.9	1.7	2	3.1	-2.5	8.0	1.7	2	3.2	-2.3	8.1	1.7	2
Lig5	3.1	-3.7	10.7	1.8	2	2.4	-4.3	5.1	1.8	2	4.1	-0.7	8.5	1.9	3	3.8	-1.1	8.5	1.9	2	3.8	-0.9	8.4	1.9	2
Lig6	3.5	-3.6	9.7	1.7	2	2.9	-6.8	6.8	1.7	2	3.7	-3.0	10.3	1.8	2	3.2	-3.4	9.3	1.7	2	3.3	-3.3	9.5	1.7	2
All	3.6	-9.0	11.7	1.8	2	3.2	-8.8	7.8	1.8	2	3.8	-7.5	12.3	1.8	3	3.4	-8.9	10.9	1.8	3	3.5	-8.7	11.2	1.8	3

Table 4. Mean absolute, minimum and maximum difference (Mad, Min, Max; in kJ/mol) between various charge sets and the QM charges for the sum of the ligand–protein electrostatic interaction energy and the generalised Born solvation energy of the simulations of Gal3. A negative sign indicates that the charge set gives more negative energies than the QM charges. In addition, the average (Av) and maximum distance (Md) at which the residue-wise cumulative energy difference is converged to within 4 kJ/mol are given. The last line gives the average, minimum or maximum over all ligands.

	Amber					Aver					xAvESP0					xAvESP1					xAvESP2				
	MAD	Min	Max	Av	Md	MAD	Min	Max	Av	Md	MAD	Min	Max	Av	Md	MAD	Min	Max	Av	Md	MAD	Min	Max	Av	Md
Lig2	3.0	0.7	8.2	2.1	3	2.5	0.1	7.8	2.1	3	2.6	0.1	9.1	2.1	3	2.5	0.2	9.0	2.1	3	2.5	0.2	9.0	2.1	3
Lig3	2.3	0.1	8.7	2.0	2	1.7	0.1	5.5	2.1	3	2.7	0.0	8.1	2.0	2	2.8	0.2	7.5	2.0	2	2.7	0.2	7.6	2.0	2
Lig4	3.0	0.1	6.4	2.1	3	2.7	0.1	7.2	2.1	3	3.3	0.1	7.0	2.1	3	3.2	0.0	7.0	2.1	3	3.2	0.0	7.0	2.1	3
Lig5	2.0	0.1	5.2	2.1	3	2.1	0.3	5.1	2.0	2	2.9	0.5	6.2	2.2	3	2.8	0.6	6.3	2.1	3	2.8	0.6	6.2	2.1	3
Lig6	3.6	0.2	8.6	2.1	3	3.0	0.2	9.4	2.0	2	3.6	0.0	7.4	2.1	3	3.5	0.1	6.9	2.1	3	3.5	0.1	6.9	2.1	3
All	2.8	0.1	8.7	2.1	3	2.6	0.1	9.4	2.0	3	3.0	0.0	9.1	2.1	3	3.0	0.0	9.0	2.1	3	3.0	0.0	9.0	2.0	3

Table 5. Binding affinities of the seven biotin analogues to avidin (kJ/mol), calculated with the MM/GBSA method with various charges. Two sets of MD simulations were performed, with either the Amber or xAvESP2 charges. MM/GBSA energies were calculated with either the Amber, xAvESP0, or xAvESP2 charge sets. MAD is the mean average deviation, when the systematic error is removed, r^2 is the squared Pearson correlation coefficient and PI is the predictive index. For comparison, experimental (Exp.) binding affinities are also included.²⁰

	Amber MD			xAvESP2 MD			Exp.
	Amber	xAvESP0	xAvESP2	Amber	xAvESP0	xAvESP2	
Btn1	-114.2±1.1	-114.6±1.2	-113.5±1.2	-117.3±1.0	-118.4±1.1	-	-85.4
						117.1±1.1	
Btn2	-102.6±1.2	-101.7±1.2	-99.7±1.2	-106.5±1.1	-	-	-59.8
					107.0±1.2	105.1±1.2	
Btn3	-102.2±0.8	-102.5±0.9	-	-105.0±0.9	-	-	-58.6
			101.4±0.9		106.3±1.0	105.1±1.0	
Btn4	-111.5±1.6	-105.3±1.6	-	-111.8±1.7	-	-	-36.8
			104.6±1.6		106.1±1.8	105.4±1.8	
Btn5	-67.8±1.4	-62.6±1.5	-61.1±1.5	-68.7±1.2	-63.6±1.4	-62.1±1.3	-34.3
Btn6	-64.5±0.7	-60.2±0.7	-60.1±0.7	-66.6±1.4	-62.4±1.4	-61.7±1.4	-20.9
Btn7	-19.7±0.5	-17.5±0.6	-17.1±0.6	-21.0±0.4	-18.8±0.5	-18.4±0.5	-18.8
MAD	14.7±0.4	14.5±0.4	14.6±0.4	15.0±0.4	15.0±0.5	15.0±0.4	
r2	0.60±0.01	0.66±0.01	0.65±0.01	0.62±0.02	0.68±0.02	0.67±0.02	
PI	0.85±0.04	0.85±0.03	0.85±0.03	0.85±0.02	0.80±0.07	0.80±0.07	

Table 6. Binding affinities of the nine inhibitors to fXa (kJ/mol), calculated with the MM/GBSA method with the Amber and xAvESP2 charge sets (both for the MD simulations and the MM/GBSA energy calculations). The quality criteria are the same as in Table 5. For comparison, experimental (Exp.) binding affinities are also included.⁵⁶

MD charges	Amber MD		xAvESP2		Exp.
	Amber	xAvESP2	Amber	xAvESP2	
C9	-65.8±1.1	-72.8±1.1	-66.1±0.9	-75.0±1.0	-46.2
C39	-48.6±0.9	-50.9±0.9	-47.8±1.0	-52.3±1.0	-27.3
C47	-56.9±1.2	-66.3±1.2	-60.8±1.1	-71.9±1.2	-46.8
C49	-62.1±1.0	-71.6±1.0	-57.5±0.9	-68.6±0.9	-41.9
C50	-52.7±0.7	-61.6±0.7	-58.6±1.1	-70.7±1.1	-46.2
C53	-58.4±1.1	-66.8±1.1	-59.1±0.9	-69.7±0.9	-44.3
C57	-52.4±0.8	-54.7±0.9	-56.8±1.3	-61.5±1.4	-38.0
C63	-55.7±1.2	-59.4±1.2	-70.0±1.1	-75.6±1.1	-37.4
C125	-62.3±1.0	-71.1±1.0	-65.6±0.9	-75.9±0.9	-43.4
MAD	4.1±0.3	3.8±0.3	4.3±0.3	3.6±0.3	
r^2	0.41±0.06	0.61±0.04	0.30±0.05	0.61±0.05	
PI	0.73±0.05	0.79±0.03	0.56±0.05	0.60±0.05	

Table 7. Comparison of calculated and experimental²⁶ S^2 order parameters for Gal3-apo, Gal3-Lac, and the difference between the two proteins. The eight different quality measures³¹ listed are the root-mean-squared-deviation (RMSD), Pearson's correlation coefficient (r^2), the mean absolute deviation (MAD), the mean absolute deviation when removing the systematic error (MADtr), the mean signed deviation (MSD), the median, the mean quote (MQ; S^2_{MD}/S^2_{NMR}), and the Q value.⁴⁹

Complex Charge set	Gal3-apo		Gal3-Lac		Difference	
	Amber	xAvESP2	Amber	xAvESP2	Amber	xAvESP2
RMSD	0.037±0.001	0.041±0.008	0.060±0.002	0.062±0.004	0.054±0.003	0.058±0.009
r^2	0.401±0.031	0.433±0.066	0.403±0.047	0.430±0.088	0.089±0.064	0.025±0.041
MAD	0.029±0.001	0.030±0.002	0.040±0.001	0.043±0.002	0.037±0.001	0.037±0.003
MADtr	0.029±0.001	0.030±0.002	0.035±0.001	0.035±0.002	0.027±0.001	0.029±0.003
MSD	-0.003±0.001	0.001±0.003	0.029±0.001	0.034±0.002	0.032±0.002	0.034±0.004
Median	0.001±0.002	0.007±0.002	0.025±0.002	0.031±0.003	0.024±0.002	0.024±0.003
MQ	0.997±0.001	1.001±0.004	1.041±0.002	1.047±0.003		
Q	0.002±0.000	0.002±0.001	0.005±0.000	0.005±0.001		

Table 8. RMSD of all back-bone atoms relative to the crystal structure (possibly with a modified ligand) for the various MD simulations with the Amber and xAvESP2 charges.

Protein	Ligand	Amber	xAvESP2
Gal3	–	0.82±0.02	0.84±0.02
	Lac	0.79±0.01	0.85±0.02
Avidin	Btn1	0.99±0.01	1.00±0.01
	Btn2	0.98±0.01	1.01±0.01
	Btn3	0.99±0.01	0.99±0.01
	Btn4	1.13±0.02	1.11±0.01
	Btn5	1.05±0.01	1.06±0.01
	Btn6	1.02±0.01	1.05±0.01
	Btn7	1.02±0.01	1.05±0.01
fXa	C9	1.16±0.01	1.01±0.01
	C39	1.06±0.01	1.08±0.01
	C47	1.20±0.01	1.08±0.01
	C49	0.99±0.01	1.05±0.01
	C50	0.98±0.01	0.96±0.01
	C53	1.15±0.01	1.08±0.00
	C57	1.22±0.01	1.06±0.01
	C63	0.97±0.01	1.18±0.01
	C125	1.08±0.01	0.97±0.01

Figure 1. The five Gal3 inhibitors (Lig1–Lig5), the seven biotin analogues (Btn1–Btn7) considered in this study (Btn1 is biotin), and the nine fXa inhibitors (C9–C125).

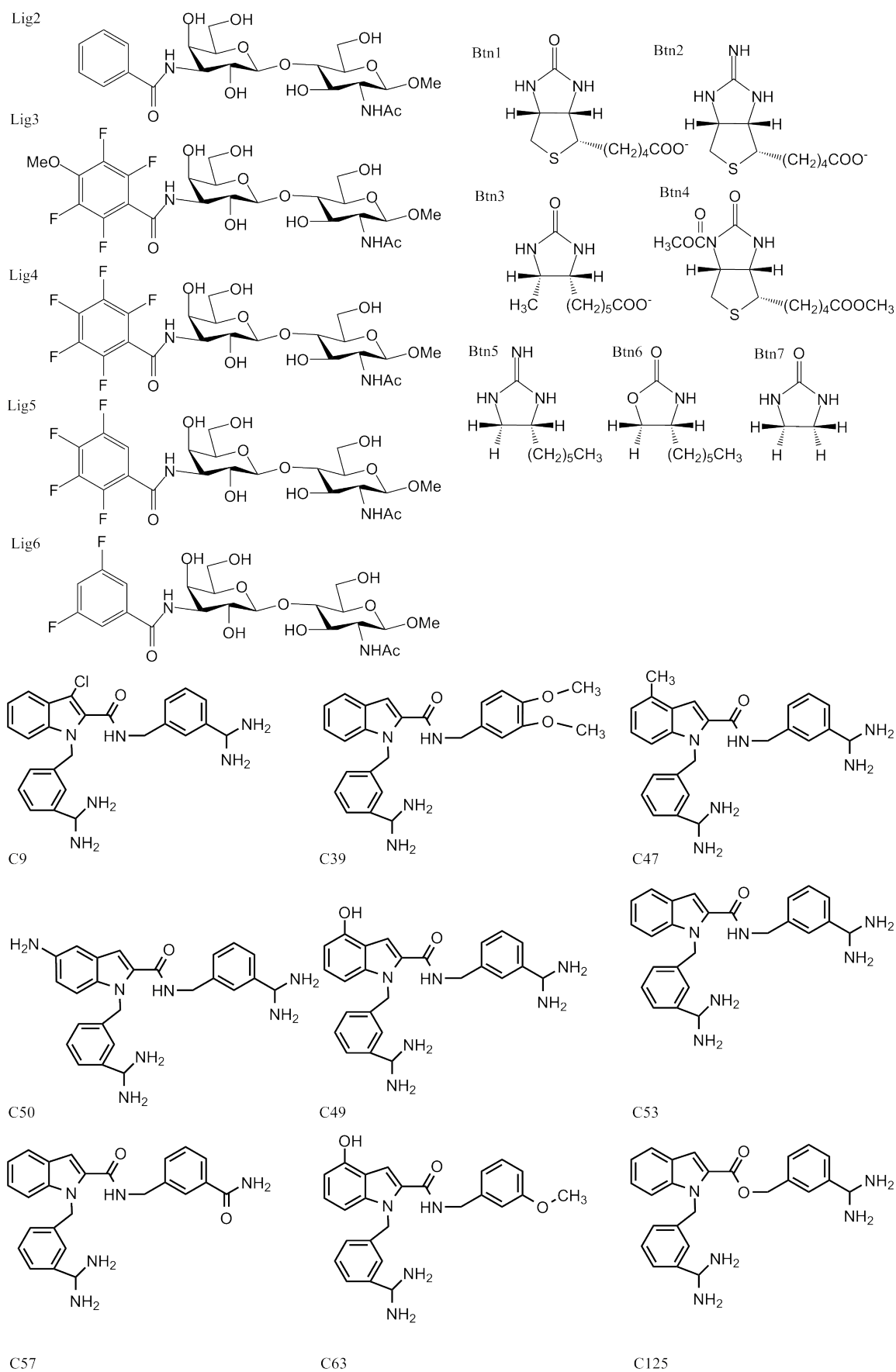


Figure 2. The correlation between the xAvESP0 and xAvESP1 charge sets. The charges are coloured according to the element.

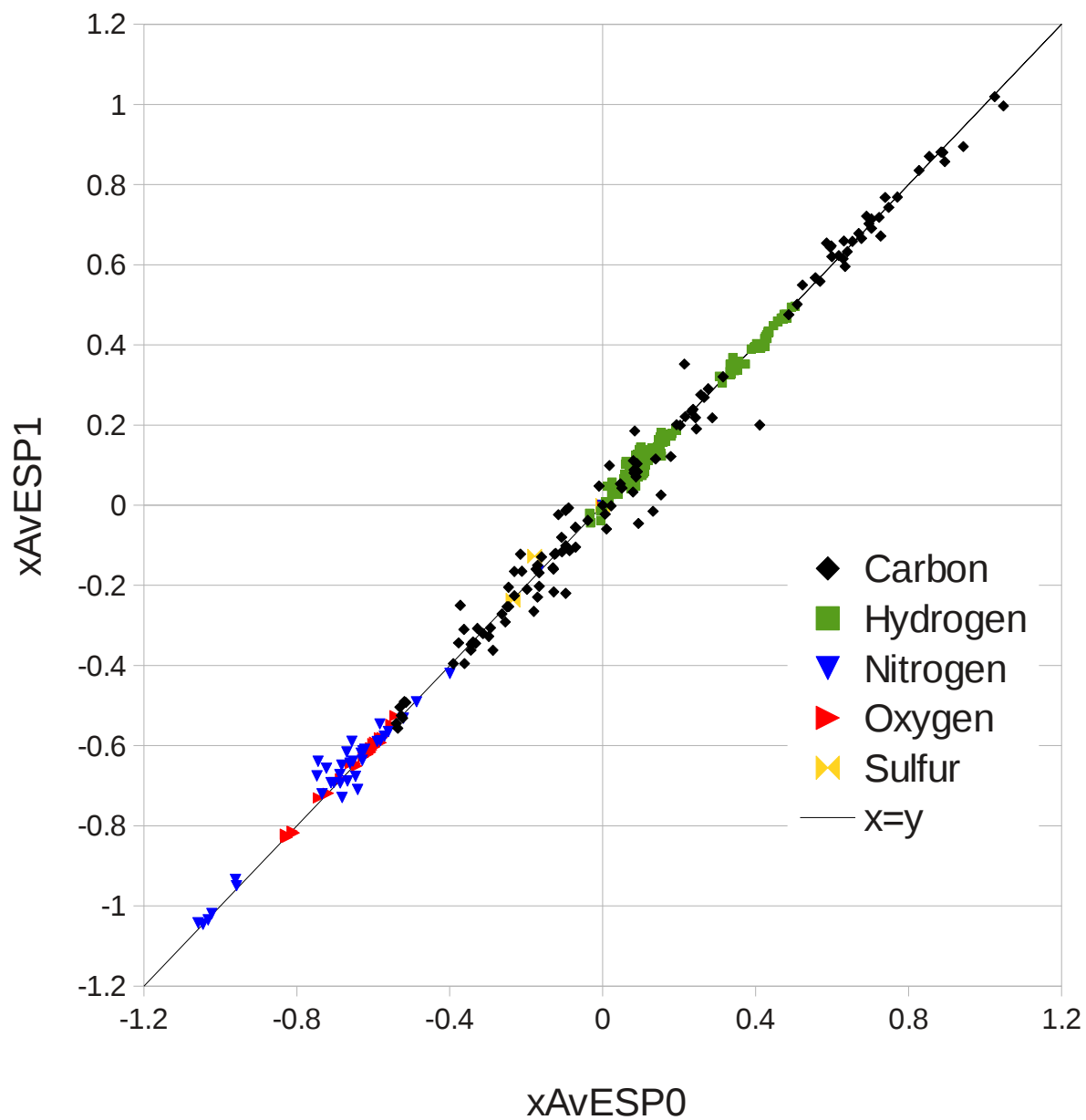


Figure 3. The correlation between the xAvESP2 and Amber charges. The charges are coloured according to the element.

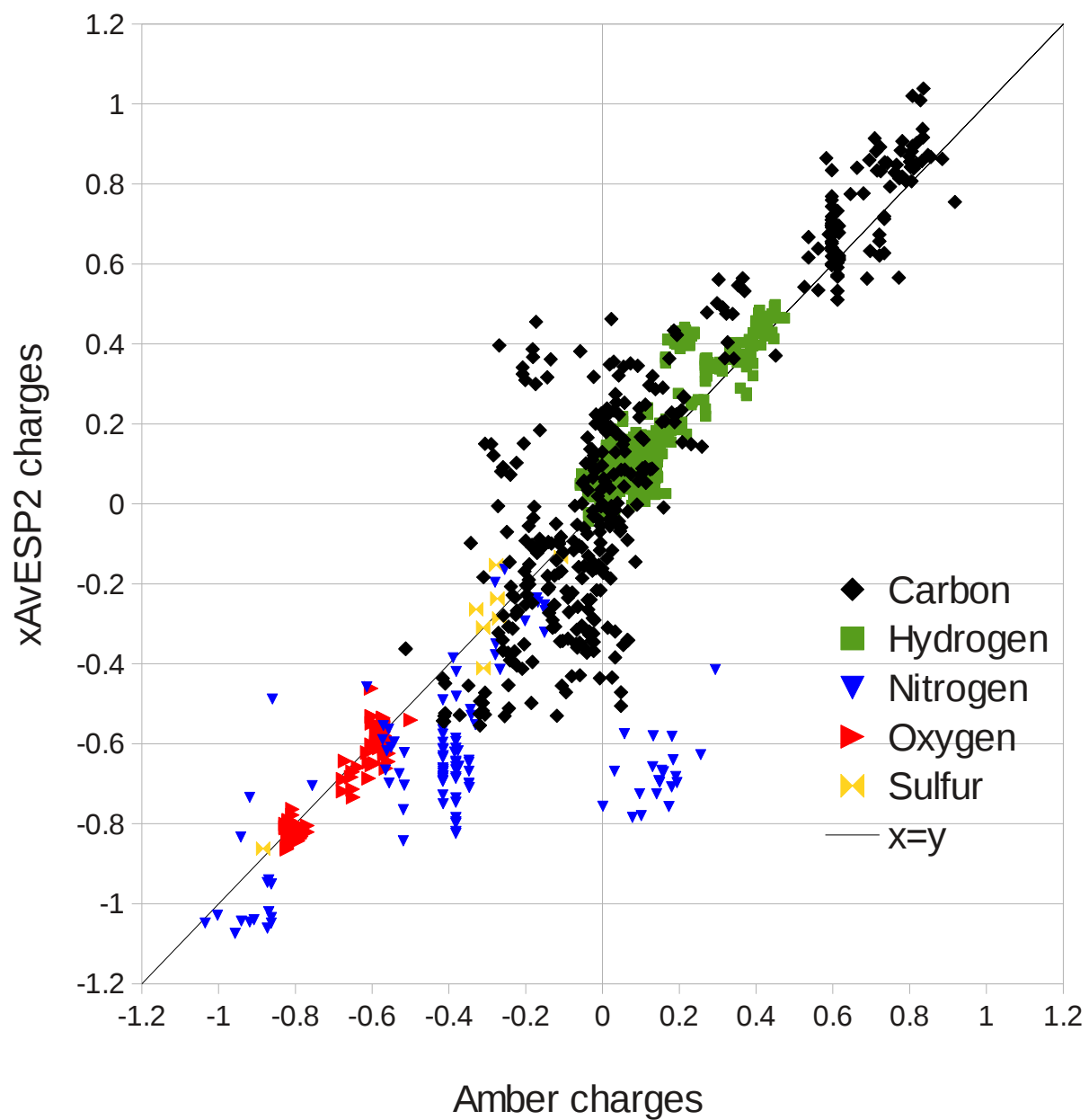


Figure 4. Total electrostatic energy within the Gal3 protein (excluding the ligand and water molecules) for the 20 snapshots of the Lig2 simulation, relative to the average energy over all snapshots for five different charge sets. a) electrostatic energies only and b) electrostatic + generalised Born solvation energies.

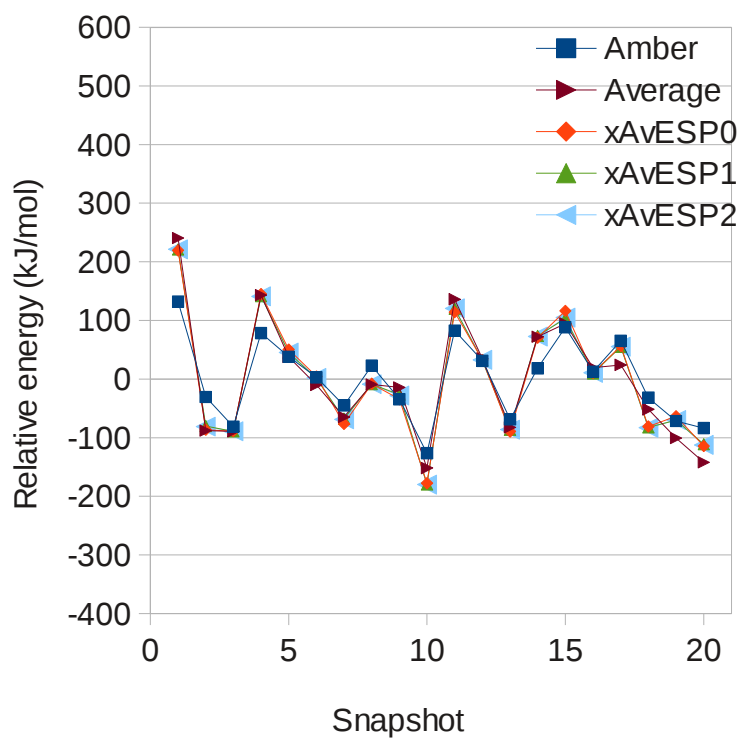
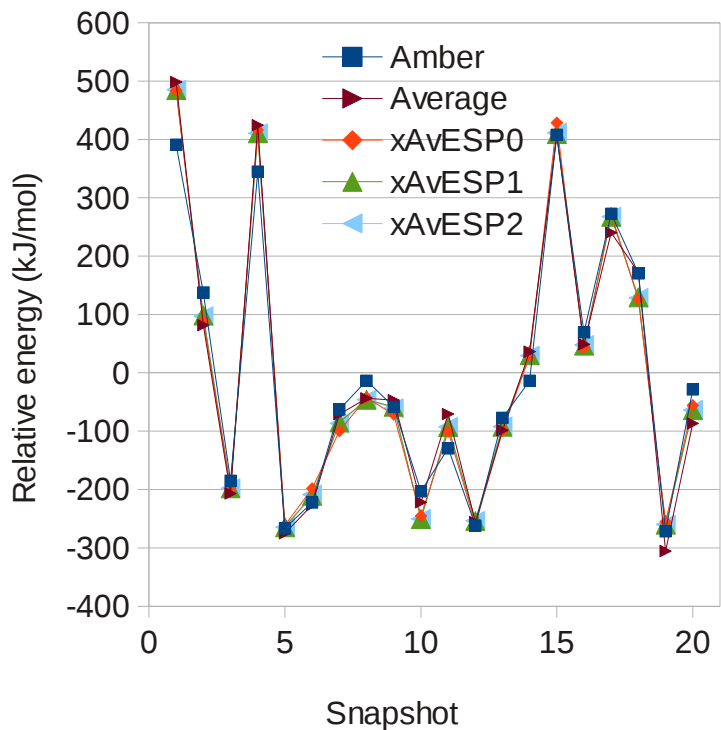


Figure 5. Distance dependence of the interaction energies between the Aver and QM charges for Lig3 bound to Gal3. Electrostatic interaction energies were calculated between Lig3 and Gal3 for both the Aver and QM charges. The differences in these interaction energies for each residue in the protein are plotted against the closest distance between the residue and Lig3 for both the individual (residue-wise) terms and for the cumulative term of all residues within the given distance to Lig3.

